HHS Public Access

Author manuscript

Dev Biol. Author manuscript; available in PMC 2018 April 01.

Published in final edited form as:

Dev Biol. 2017 April 01; 424(1): 1–9. doi:10.1016/j.ydbio.2017.02.013.

Repeated removal of developing limb buds permanently reduces appendage size in the highly-regenerative axolotl

Donald M. Bryant[1], **Konstantinos Sousounis**[1,2], **Johanna E. Farkas**[3], **Sevara Bryant**[1], **Neng Thao**[1], **Anna R. Guzikowski**[1], **James R. Monaghan**[3], **Michael Levin**[2,4], and **Jessica L. Whited**[1,2]

[1]Department of Orthopedic Surgery, Brigham & Women's Hospital, Harvard Medical School, Cambridge, MA, 02139, USA

[2]Allen Discovery Center at Tufts, Medford, MA, 02155, USA

[3]Department of Biology, Northeastern University, Boston, MA, 02115, USA

[4]Tufts Center for Regenerative and Developmental Biology, Medford, MA, 02155, USA

Abstract

Matching appendage size to body size is fundamental to animal function. Generating an appropriately-sized appendage is a robust process executed during development which is also critical for regeneration. When challenged, larger animals are programmed to regenerate larger limbs than smaller animals within a single species. Understanding this process has important implications for regenerative medicine. To approach this complex question, models with altered appendage size:body size ratios are required. We hypothesized that repeatedly challenging axolotls to regrow limb buds would affect their developmental program resulting in altered target morphology. We discovered that after 10 months following this experimental procedure, limbs that developed were permanently miniaturized. This altered target morphology was preserved upon amputation and regeneration. Future experiments using this platform should provide critical information about how target limb size is encoded within limb progenitors.

Keywords

limb; development; regeneration; axolotl; morphogenesis; growth

INTRODUCTION

From fertilization to cleavage, development, and adulthood a specific and robust developmental program ensures proper animal form. Organs and appendages are grown in a stereotypical and orderly fashion, following a programed timeline that is largely invariant

[*]*Corresponding author*: Jessica L. Whited, PhD, 65 Landsdowne St. Room 283, Cambridge, MA 02139, (617)-768-8422, jwhited@bwh.harvard.edu.

within a given species. Appendage development, for instance, is intimately connected to progenitor cell distribution, growth factors, and patterning mechanisms (reviewed in (1–4), for example, (5–9)). Over the course of organismal growth, animals calibrate the size of their appendages to the size of their bodies. Once these structures have stopped growing, active molecular processes ensure they are not pathologically overridden; for example, size/growth control is also a key issue in cancer.

Within a species, a relatively constant ratio exists for appendage size versus, for instance, overall body length or height (reviewed in (10, 11)). Permutations of this program have been uncovered in zebrafish by screening for mutants with altered fin:body ratios (12). This work has uncovered a role for potassium channels in regulating the appendage-body size relationship, but the mechanisms connecting changes in membrane potential to overall appendage size remain murky. Because localized overexpression of potassium channels is sufficient to instigate nearby tissue overgrowth, the control of appendage size may largely be controlled at the local level (12). The intrinsic ability of the tissue itself to dictate the size of the growing organ was also highlighted in a transplantation experiment with two different sized salamanders where their limb buds were swapped. The limb buds of the larger species produced large limbs on the smaller hosts, and the limb buds of the smaller species produced small limbs on the large hosts (13). This result is consistent with the idea that limb buds are autonomous units programmed with the information necessary to produce the appropriately-sized appendage for the animal that will ultimately grow into an adult. The experiment also suggests that information from the host's body—for example, information about its size—cannot override the pre-defined growth determinant of the graft. However, in these inter-species chimeric experiments communication between the graft and host cells may be inhibited due to tissue incompatibilities at the molecular level or even hindered by epigenetic differences. We wanted to develop a model that decouples appendage size to body size within the same species in order to further explore this fundamental relationship in the future.

Inducing an organism to grow a different sized appendage than what was initially programmed is challenging. Surgical manipulation is not a viable option for most vertebrates, as they only have the ability to induce limb buds during embryonic development. Salamanders, however, are a uniquely tractable model for this line of research because they are highly-regenerative animals that can remake a lost limb throughout their lives. This also raises the possibility that salamanders are capable of growing a limb repeatedly when challenged, a phenomenon that has been already documented in other regeneration model systems (14, 15). In axolotl embryos, cells within the "pre-bud limb rudiments" have been found to behave as a homogeneous field insofar as removal of subsets of these cells can still lead to later development of normal limbs (16). Young larvae, called hatchlings, have *bona fide* limb buds outgrowing from the body within 5–6 days post-hatching (stage 44 according to (17)). Limb buds can be surgically removed while still rudimentary and exhibiting no outward signs of differentiation. We hypothesized that if we could temporally delay the first iteration of a developed, patterned limb, by repeatedly removing the limb bud, we might defeat the robust developmental blueprint and generate limbs with altered target morphologies. We discovered that this approach permanently reduces the limb size of axolotls, decoupling appendage size and body size in a tetrapod.

This novel example of a permanent alteration of target morphology (the final shape and size that an appendage or organ grows or regenerates to) establishes a molecularly-tractable model in which to uncover the mechanisms that underlie appendage size, and more broadly, to begin to investigate the extent to which default anatomical patterns can be re-specified without genomic editing.

RESULTS

Repeated limb bud removals for eleven weeks results in distinct truncation and loss of anterior autopodial elements

To examine the consequences of delayed limb formation on morphological outcomes in the forelimb, we repeatedly performed bilateral forelimb bud removal starting from newly hatched axolotls and continued the removal as the animals repeatedly regrew this bud-like structure (Figure 1A). We designed the experiment such that we started with a large cohort of newly-hatched siblings, and we dropped groups of animals out of the repeated bud removal protocol on designated days. Dropping the animals out allowed them to develop forelimbs if they were capable. At the end of the experiment, we analyzed the morphology and size of all the forelimbs in the entire cohort. This strategy allowed us to query the effect of repeated regrowth of forelimbs throughout this time course and to track the morphological results according to when the cohorts were allowed to grow that first limb. We observed that 78% of forelimbs that grew following as many as 10 bud removals were often patterned normally (n=72/92 forelimbs from a total of 46 animals across all dropped out groups, Figure 1B–B', Supplementary Table 1). Some limbs displayed anatomical defects in the autopod with truncated digits or reduced digit numbers (Figure 1B–B', Supplementary Table 1). Notably, the patterning abnormalities that we observed tended to be along the anterior side of the limb. All of the unchallenged forelimbs of sibling controls formed correctly (n=24/24 control forelimbs from 12 animals examined).

Prolonged repeated removal of forelimbs results in amelia and the formation of miniaturized limbs

Intrigued by our findings, we decided to extend the experiment to determine if axolotls could generate correctly patterned limbs even if they were challenged to do so as many as 10 months post-hatching (Figure 1C). Typically, animals could form a bud-like structure within 8 to 9 days after removal of the previous bud. However, we noticed that animals began failing to generate these structures as the study progressed (Figure 1D–F). In fact, we observed a rapid loss in the ability of axolotls to form these structures between 200 and 300 days post-hatching, with more than half of the limbs failing to generate any bud-like tissue when delayed to ~300 days post-hatching (Figure 1G). These data indicate that even the highly-regenerative axolotl has a limited, albeit impressive, ability to generate a limb bud repeatedly.

As most of the animals in our study were losing the ability to generate even a bud-like structure, we decided to allow limb formation to progress in these animals at 313 days pos-thatching. Given our previous observations on limb abnormalities in delayed limbs, we speculated that forelimbs whose development was repeatedly reinitiated for nearly a year

would have severe patterning defects. To control for defects that may arise due to age-related mechanisms, we reserved siblings at the beginning of the experiment. We did not manipulate these animals, and indeed they grew perfect limbs at the prescribed developmental time, which grew in size accordingly as the animals aged. We amputated these control siblings for the first time at 313 days post-hatching at the same plane as the animals receiving repeated bud removals (i.e. flush with the body), and as expected nearly all of them regenerated with four digits (n=24/26 normal limbs). The two control limbs that regenerated abnormally were hypomorphic and exhibited syndactyly or loss of digits. Interestingly, among the cohort of experimental animals in which we were repeatedly removing their limb bud until this 313-day time point, we observed a nearly binary result. These axolotls either failed to generate limbs entirely (n=19/32 limbs) or formed limbs that appeared morphologically normal, but substantially smaller (n=12/32 limbs), than those of their sibling controls (Figure 1H–J). Overall, the growth of both cohorts with respect to other bodily features, such as the hindlimbs, appeared comparable (Supplementary Figure 1A). Likewise, there was no significant difference in the snout-to-tail length of the animals at the end of the experiment (control: 16.2+0.4 cm, n=13; miniature: 16.5+0.3 cm, n=16; p=0.58). Thus, this operation appears to have decoupled limb size from body size and age. We found some animals in which both forelimbs were completely lost in the experiment, and thus were absent, while others lost only one forelimb, and a few grew two miniaturized forelimbs (Figure 1K).

A closer examination of forelimb skeletal elements revealed that miniature limbs formed by repeated limb bud removal possessed all of the typical bone structures, were correctly patterned, and exhibited normal ossification (Figure 2A–B’). The miniaturized limbs were also functional as axolotls were able to paddle them in response to a stimulus at the surface of their tanks (Supplementary Video 1). We wondered whether the observed reduction could be normalized as animals aged. To answer this question, we monitored the total length and width of these animals’ limbs at 66, 111, and 174 days post-procedure. “Post-procedure” refers to either a proximal amputation of naive sibling control forelimbs (i.e., the first time these animals were manipulated) or the last removal of the bud-like structure in the experimental animals. Measurements are diagrammed in Figure 2C. Both control and miniature limbs grew substantially from 66 to 174 days post-procedure (Figure 2D–F). However, this increase in growth appeared to plateau after 111 days post-procedure in both groups, and miniature limbs were still significantly smaller than controls despite 174 days of growth (around six months). Furthermore, these limbs remained miniaturized even though the animals were allowed to grow for over two years after they first formed a limb (Supplementary Figure 2). Together, these data suggest that the reduction in size was not transient, and these animals were not undergoing compensatory growth.

Although we amputated the limbs of control siblings at the same plane as animals receiving repeated bud removals, we performed additional experiments to rule out the possibility that the repeated bud removal results we obtained may be attributable to the surgical procedure. Specifically, we sought to rule out any possibility of the cutting plane having been “too close” to the body to support the growth of a full-sized limb. Therefore, we performed an experiment whereby within individual animals, one completely-developed forelimb was amputated flush with the body, while the contralateral completely-developed forelimb was amputated at the mid-stylopod (mid-humerus) level (several millimeters distal to the body

wall). In all cases (n=8 animals/16 limbs), both limbs were able to regenerate to form digits (Supplementary Figure 1B,C). We did not observe a significant difference in zeugopodial width or zeugo-autopodial length between limbs amputated at the girdle-level and limbs amputated at the mid-stylopodial level (Supplementary Figure 1B,C and Supplementary Table 2, $p>0.05$). Interestingly, we did observe a significant difference in stylopodial width between regenerates resulting from the different amputation planes, but the stylopodium was larger (wider) in limbs amputated at the girdle level relative to limbs amputated mid-humerus (Supplementary Figure 1B,C and Supplementary Table 2, $p<0.01$).

In addition to absolute size, we were also interested in whether the miniaturized limbs had proper dimensionality relative to sibling control limbs. When normalized to total limb length, we found that zeugopodial width in miniature limbs was not significantly different than that of control limbs (Figure 2G, $p>0.05$). However, we found that the ratio of stylopodial width to total limb size and zeugopodial width was smaller in miniature limbs relative to controls (Figure 2H–I, $p<0.001$). Taken together, our data suggest that among the animals competent to form a completely patterned limb for the first time after repeated surgical removals for nearly a year post hatching, they are unable to achieve appropriate size appendage.

We also performed a second experiment in which the bud removals occurred more frequently than the first experiment (average of 7 days between removals versus 8 days). As with our first experiment, we observed that the shorter interval between bud removals produced similar patterning defects (e.g. digit truncation), limb loss, and miniature limbs, but the limb loss and miniature limbs manifested after fewer bud removals (data not shown). Thus, shortening the window between removals appears to be sufficient to drive the system to an altered state more quickly.

Miniaturized forelimbs are nerve-deficient

We next sought to determine why these limbs displayed such a dramatic reduction in size. One mechanism by which the size disparity could have arisen is by a reduction in the amount of nerves in the limb. In humans, injury of the nerves in the brachial plexus during birth often leads to the formation of a limb that is smaller than its contralateral non-injured counterpart; surgical repair of the nerves can reduce the size disparity between injured and non-injured limbs (18). Denervation of amphibian limbs during development results in a reduction in limb size (19). Moreover, denervation of the salamander limb after the blastema has formed also leads to the formation of a miniaturized regenerate limb (20). More broadly, this system can be used to study the contribution of the nervous system to the plasticity of regenerative program with respect to pattern. To test the possibility that miniaturized limbs are deficient in nerves, we stained cross-sections (Figure 3A) of control and miniature limbs with the nerve-specific β-III tubulin antibody (Figure 3B). As expected, miniature limbs were innervated. However, they had a reduction in the area covered by nerves. When the surface area covered by nerves was normalized to cross-sectional area, we found that miniaturized limbs still had significantly fewer nerves relative to control limbs (Figure 3C; $p<0.01$, n=4 per group). We also analyzed the relative amount of muscle and bone in control versus miniature limbs, and we did not observe significant differences in either tissue

(Figure 3D–E). These findings suggest that a lack of nerves, but not muscle or bone, may contribute to the reduction in limb size that we observed.

Miniaturized limbs give rise to miniaturized limbs after amputation

Integrating appendage/organ size and body size are critical for the proper homeostasis of an organism (21–23). How does an animal's robust regeneration program relate to the starting conditions established for complex structures during embryogenesis? Because the animals with small limbs were the same age and size of their sibling controls, the miniaturized limb model afforded us the opportunity to ask how the regeneration program determines what size limb it should regenerate. If the blastema calculates the size of the limb it forms based on local tissue, or if the target morphology is imprinted to surviving cells, then one would predict that miniaturized limbs would regenerate limbs that are smaller relative to control limbs. Conversely, if a systemic mechanism determined by the organism's normal genome controls regenerate limb size, one would predict miniaturized limbs might regenerate limbs whose size was matched to the animal's body/trunk, and therefore larger than the precursor miniature limb and similarly sized to controls. Following amputation, miniature limbs were able to give rise to morphologically mature blastemas that were about half the size of their control counterparts at 23 days post-amputation, suggesting that they were regeneration-competent and possessed enough nerves to drive regeneration (Figure 4A). Furthermore, at 11 weeks post-amputation, most miniaturized forelimbs (83%) regenerated new limbs with four discernible digits (Figure 4B, n=10/12 limbs from 10 animals). A similar percentage of control forelimbs (85 %) regenerated limbs with a full set of digits (Figure 4B, n=22/26 limbs). Interestingly, all of the fully-regenerated miniaturized limbs appeared to have compromised ossification relative to their control counterparts, and several had incomplete ulna formation (Figure 4B', n=4 regenerated limbs with four digits but incomplete ulna formation), indicating that regeneration was not always complete. Regardless, the newly-formed limbs that regenerated from miniature limbs were significantly smaller than limbs regenerated from control siblings of the same age (Figure 4C–D, $p<0.001$), demonstrating that the miniaturized limb is a permanent condition. This result further suggests that local tissue size or cell predisposition is a primary driving force for size determination during limb regeneration. These results are consistent with the species-specific limb size maintenance in regeneration seen in Pescitelli and Stocum's cross-species blastema transplantations and parallel Twitty and Schwind's findings that heteroplastically transplanted limb buds develop in size according to the species from which they are derived (13, 24).

DISCUSSION

The described model has one unique feature and a simple outcome. It does not involve chemicals, wounding of the body cavity or transgenesis but only relies on the repeated and timely removal of limb buds. The result is binary: limbs will be remarkably small compared to the body size or they will never regrow. This unique platform can be used to study the mechanisms that dictate the size of an appendage.

Our results are consistent with a previous experiment by Maden and Goodwin in which limb buds were removed from hatchling axolotls upon primary presentation (25). Both our report

and this earlier report find that axolotls can completely compensate for the loss of that first instance of limb bud, and that all axolotls that underwent one round of bud removal grew completely normal limbs (25). However, our study interrogates this concept further to test the ability of axolotls to make a limb following additional removal of the bud-like structure, and effectively forcing the animals to grow limbs at later times in life. Up to a certain point (our “short-term bud removals”), most of the limbs challenged in this way did generate a normal limb (78%). However, a fraction of limbs (22%) were indeed compromised in their morphogenesis, as evidenced by distal anterior patterning defects. After this point (our “long-term bud removals”), our experiment uncovered a miniaturization effect.

We can speculate several possible explanations for the defects seen in our model. One possibility is that the continuous mobilization and proliferation of limb progenitor cells exhausts them. This reduction in number may induce a weaker response that makes a miniaturized limb or is not sufficient to start the process. In terms of the miniaturization phenotype, it is also possible that these limbs have some impairment in their ability to grow to a normal size after they are initially patterned. However, future studies are needed to determine the relative contributions that progenitor cell activation and post-patterning growth make during the process of limb miniaturization. A second, though not mutually exclusive, possibility is that some disconnection exists between the progressed state of the body and the developing appendage which must be integrated. This possibility is suggested by the sparser innervation of the miniature limbs we observed in animals that grew their first limbs at nearly one year of age. Future experimentation may uncover whether in this scenario axons are perhaps permanently pruned due to the missing target area, and whether cell bodies situated outside the limb may be reduced in number. Although beyond the scope of the present study, the contribution of nerve deficiency to the miniaturization that we observed could be tested by combining nerve deviation experiments with repeated bud removal. If deviation of a nerve to a limb field that is challenged by repeated bud removal results in the formation of larger limbs, then these data would provide strong support for a miniaturization model based on nerve deficiency. Future work may use this model to determine the molecular mechanisms underlying the diminishment of limb bud growth over time.

A decline in the fidelity of limb regeneration has also been documented to occur in axolotls following metamorphosis, which can be induced in these neotenic animals by thyroxine administration (26). However, the defects observed in that study were primarily loss of carpals (93%) and loss of the posterior-most digit (digit IV, 60%) and are therefore distinct from those observed in our study. Indeed, the deficiencies in metamorphic axolotls may more readily point to compromised signaling from the posterior signaling center. Our miniaturization and appendage loss effects are reminiscent of key findings in studies by Thornton (1943) and Alberch and Gale (1983) (27, 28). When mitosis is blocked in axolotl limb buds by colchicine application, smaller limbs develop (27); however, when colchicine is applied after limb amputation, regeneration is blocked (28). Notably, the digit loss effects are different from what we observed, which might be due to the different effects each treatment has on the progenitor pool.

An exciting outcome of this research has been the experimental decoupling of limb size from body size. The regenerative model is powerful for studying these relationships, and for understanding how organisms allocate growth resources over their life spans. Future studies in axolotl using this model could further reveal molecular mechanisms that govern the coupling of appendage size to body size.

EXPERIMENTAL PROCEDURES

Repeated bud removal

All animal experimentation was performed in accordance with the Harvard Medical School's Institutional Animal Care and Use Committee's guidelines and under animal experimentation protocol #04160. Leucistic axolotls (*Ambystoma mexicanum*) were used throughout the study. All animals used were bred in-house and raised in individual containers for the duration of the experiment. Animals were separated before or shortly after hatching and kept in separate enclosures for the entire experiment. For limb bud removals, animals were anesthetized in 0.1% tricaine and recovered in 0.5% sulfamerazine overnight.

The data presented in our study is from 75 animals (150 limbs) that survived for the duration of experimentation. Among these 75 animals, 13 animals served as controls, and the remaining 62 animals underwent repeat bud removal procedures. These 62 animals were split into two groups: short-term bud removal (i.e. up to 10 removals) with random animal dropout and long-term bud removal (i.e. 36 bud removals) without dropout (Figure 1A,C). There were a total of 46 animals (92 limbs) in the short-term bud removal study and 16 animals (32 limbs) in the long-term bud removal study. The first limb buds were removed at approximately Stage 46 (17). Unperturbed siblings were used as a control to ensure that there was not an unusually high rate of developmental limb deformities for the short-term study and were later amputated as controls for animals in the long-term bud removal study.

For the short-term bud removal study (Figure 1A), limb buds were removed every 8 days on average. The removal window sometimes varied depending upon the ability of the animals to form a properly sized limb bud, but the time window did not vary by more than one day for the first 10 bud removals (e.g. no longer than 9 days between bud removals). After each bud removal, 3 – 6 animals (6 – 12 limbs) were dropped out of the study and allowed to regenerate. Thus, a minimum of 6 limbs were assayed for defective regeneration in each dropout group. The sample sizes and hypomorphic phenotypes (e.g. digit loss) for each dropout group are presented in Supplementary Table 1.

For the long-term bud removal study (Figure 1C), we performed 36 rounds of forelimb bud removal on 32 limbs (16 animals) without dropout. Bud removals were performed every 8 – 9 days on average, although we sometimes had to wait for up to 12 days for the buds to fully reform and to ensure a consistent bud removal. This lengthened window was observed as the animals appeared to reach adulthood (i.e. around 8 – 9 months of age). The last bud removal for this experiment was performed at approximately 313 days post-hatching (i.e. 301 days after the initial bud removal) (Figure 1C). At the same time, we performed proximal amputations (i.e. girdle-level) on both forelimbs of the 13 sibling control animals to control for age-associated regenerative defects (Figure 1C). From this point on, we allowed the

limbs to fully form. The regeneration experiments described in Figure 4 were performed on the limbs that fully developed after the 36th bud removal (miniature limbs) and proximal full-limb amputations (controls).

Sex-related animal information

For experiments involving quantification and analysis of miniaturized limbs (Figure 1D–K, Figures 2–4), the animals used were approximately 1 – 1.5 years in age (range accounts for aging during regeneration experiments). For the control animals in Figure 1D–K and Figures 2–4, 6 out of the 13 animals used were females, and the remaining 7 animals were males; 10/16 of the animals from the miniaturized limb group were females, and the remaining 6 animals were males. Because the animals used for Figure 1B,B' were within the first 3 months of hatching, we could not confidently determine the exact sex of these animals. In axolotls, the identification of specific sex depends on the clear distinction between size of the external tissue adjacent to the cloaca (males develop a large and obvious cloacal gland), and the difference between males and females is not typically clear until the animal is around 6–12 months of age.

Microscopy

All whole mount and skeletal preparation images were acquired on a Leica M165 FC stereomicroscope, and measurements were acquired with the Leica Application Suite software. Amputated limbs were imaged in 1X PBS. Skeletal preparations were performed according to (13) and imaged in a 3:1 glycerol to 1% potassium hydroxide solution. Animals in Figure 1D–F were imaged ventrally in 0.1% tricaine, and animals imaged in Figure 1H–J were imaged laterally. For clarity, images of limbs were sometimes mirrored.

Skeletal preparations

Limbs were stained with Alcian blue/Alizarin red according to (29). Briefly, limbs were fixed in 95 % ethanol overnight. Limbs were then incubated in acetone overnight and then transferred to Alcian blue/Alizarin red staining solution. Samples were then cleared in a 1 % potassium hydroxide solution and stored in glycerol.

Histology

Tissue was harvested and fixed in 4% paraformaldehyde in PBS, brought through a sucrose series (beginning with incubation in 5 % sucrose and ending with a final 30 % sucrose equilibration step), embedded in OCT, and flash-frozen. Frozen sections were acquired via cryostat at 16 μm. Immunohistochemistry with the mouse monoclonal (IgG_{2a}) β-III tubulin antibody (1:50 of 0.5 mg/mL stock, R&D Systems: MAB1195, LOT: HGQ0113121, Clone # TuJ-1) was performed as in (30). Goat anti-mouse IgG_{2a} coupled to Alexa-fluor 488 (1:300, Life Technologies: A21131), and phalloidin conjugated to Alexa-fluor 594 (1:40, Life Technologies: A12381) were used secondarily. Samples were incubated in DAPI (1.4 μmol/L) for 10 minutes, and slides were mounted with hydromount. Fluorescent images were acquired on an Olympus 1X71 microscope and processed with MetaMorph Basic (V7.7.0.0) software, and low magnification images were manually stitched together. ImageJ was used to add scale bars, adjust color balance, and quantify images. For quantification of

innervation in Figure 3C, a common threshold for fluorescence emitted by nerves was applied to all images using ImageJ. The “Analyze Particles” function within ImageJ was used to measure surface area covered by nerves. Total cross-sectional area of sections was also measured with ImageJ as with muscle and bone.

Statistical Analyses

All data are presented as mean +/− sem. For the analysis in Figure 2, animals were imaged laterally and total limb length, stylopod width, and zeugopod width were measured. For animals with two limbs, we averaged each of the above values across both limbs to generate a measurement for each animal. If an animal had one limb, then only that limb was used to generate measurements for that particular animal. This approach was taken so that each animal would have equal weight in the analysis. Animals with no limbs were not considered in these analyses. A two-way ANOVA was conducted followed by post-hoc analyses with Bonferroni’s Multiple Comparison’s Test. Statistical analyses were conducted using GraphPad Prism 7, R, and Excel. A two-tailed homoscedastic t-test was used to compare innervation, muscle area, and bone area between control limbs and miniature limbs in Figure 3C–E. The limbs in Figure 4 were harvested and imaged dorsally. For Figure 4, regenerate lengths and widths were averaged across left and right forelimbs if an animal regenerated both; if an animal only regenerated one limb, then only that limb’s measurements were used (i.e. the measurements were not averaged for non-regenerating limbs). Limbs that did not regenerate to the digits stage were not quantified since these limbs could not be measured with a high degree of confidence. For Figure 4C–D, a two-tailed homoscedastic t-test was used to assess statistical significance. A two-tailed paired t-test was used to compare regenerates resulting from the girdle-level amputation and mid-stylopodial amputation in Supplementary Table 2.

Supplementary Material

Refer to Web version on PubMed Central for supplementary material.

Acknowledgments

This work was supported by the Howard Hughes Medical Institute [Gilliam Fellowship to D.M.B.], the American Academy of Neurology [Medical Student Summer Research Scholarship to S.B.], the March of Dimes [Basil O’Connor Award to J.L.W.], the National Institutes of Health [DP2HD087702 to J.L.W.], the Paul G. Allen Family Foundation [Frontiers Group to K.S., J.L.W., and M.L.] and Brigham & Women’s Hospital. We thank Frank Davis, Emily Pate, and Margarete Diaz Cuadros for assistance with experimental procedures, and we thank William Ye, Athylia Paremski, Colleen Carmody, Samantha Furgason, and Soyisha Sylvain for animal care. We thank Victor Luria, Fernando Camargo, Cliff Tabin, and members of the Whited lab for helpful comments.

References

1. Sheeba CJ, Andrade RP, Palmeirim I. Getting a handle on embryo limb development: Molecular interactions driving limb outgrowth and patterning. Semin Cell Dev Biol. 2015
2. Chen H, Johnson RL. Dorsoventral patterning of the vertebrate limb: a process governed by multiple events. Cell Tissue Res. 1999; 296(1):67–73. [PubMed: 10199966]
3. Tabin C, Wolpert L. Rethinking the proximodistal axis of the vertebrate limb in the molecular era. Genes Dev. 2007; 21(12):1433–1442. [PubMed: 17575045]

4. Tickle C. Making digit patterns in the vertebrate limb. Nat Rev Mol Cell Biol. 2006; 7(1):45–53. [PubMed: 16493412]
5. Riddle RD, Johnson RL, Laufer E, Tabin C. Sonic hedgehog mediates the polarizing activity of the ZPA. Cell. 1993; 75(7):1401–1416. [PubMed: 8269518]
6. Zhu J, et al. Uncoupling Sonic hedgehog control of pattern and expansion of the developing limb bud. Dev Cell. 2008; 14(4):624–632. [PubMed: 18410737]
7. Yu K, Ornitz DM. FGF signaling regulates mesenchymal differentiation and skeletal patterning along the limb bud proximodistal axis. Development. 2008; 135(3):483–491. [PubMed: 18094024]
8. Kawakami Y, et al. WNT signals control FGF-dependent limb initiation and AER induction in the chick embryo. Cell. 2001; 104(6):891–900. [PubMed: 11290326]
9. Cooper KL, et al. Initiation of proximal-distal patterning in the vertebrate limb by signals and growth. Science. 2011; 332(6033):1083–1086. [PubMed: 21617075]
10. Lui JC, Baron J. Mechanisms limiting body growth in mammals. Endocr Rev. 2011; 32(3):422–440. [PubMed: 21441345]
11. Gould SJ. Allometry and size in ontogeny and phylogeny. Biol Rev Camb Philos Soc. 1966; 41(4): 587–640. [PubMed: 5342162]
12. Perathoner S, et al. Bioelectric signaling regulates size in zebrafish fins. PLoS Genet. 2014; 10(1):e1004080. [PubMed: 24453984]
13. Twitty VC, Schwind JL. The growth of eyes and limbs transplanted heteroplastically between two species of Amblystoma. J Exp Zool. 1931; 59(1):61–86.
14. Yun MH, Davaapil H, Brockes JP. Recurrent turnover of senescent cells during regeneration of a complex structure. Elife. 2015; 4
15. Eguchi G, et al. Regenerative capacity in newts is not altered by repeated regeneration and ageing. Nat Commun. 2011; 2:384. [PubMed: 21750538]
16. Slack JM. Regulation and potency in the forelimb rudiment of the axolotl embryo. J Embryol Exp Morphol. 1980; 57:203–217. [PubMed: 7430930]
17. Nye HL, Cameron JA, Chernoff EA, Stocum DL. Extending the table of stages of normal development of the axolotl: limb development. Dev Dyn. 2003; 226(3):555–560. [PubMed: 12619140]
18. Bain JR, et al. Limb length differences after obstetrical brachial plexus injury: a growing concern. Plast Reconstr Surg. 2012; 130(4):558e–571e.
19. Dietz FR. Effect of peripheral nerve on limb development. J Orthop Res. 1987; 5(4):576–585. [PubMed: 3500294]
20. Singer M, Craven L. The growth and morphogenesis of the regenerating forelimb of adult Triturus following denervation at various stages of development. J Exp Zool. 1948; 108(2):279–308. [PubMed: 18873226]
21. Umulis DM, Othmer HG. Mechanisms of scaling in pattern formation. Development. 2013; 140(24):4830–4843. [PubMed: 24301464]
22. Stevens CF. Control of organ size: development, regeneration, and the role of theory in biology. BMC Biol. 2015; 13:14. [PubMed: 25706761]
23. Stanger BZ. The biology of organ size determination. Diabetes Obes Metab. 2008; 10(Suppl 4):16–22.
24. Pescitelli MJ Jr, Stocum DL. The origin of skeletal structures during intercalary regeneration of larval Ambystoma limbs. Dev Biol. 1980; 79(2):255–275. [PubMed: 7000577]
25. Maden M, Goodwin BC. Experiments on developing limb buds of the axolotl Ambystoma mexicanum. J Embryol Exp Morphol. 1980; 57:177–187. [PubMed: 7430928]
26. Monaghan JR, Stier AC, Michonneau F, Smith MD, Pasch B, Maden M, Seifert AW. Experimentally induced metamorphosis in axolotls reduces regenerative rate and fidelity. Regeneration. 2014; 1(1):2–14. [PubMed: 27499857]
27. Alberch P, Gale EA. Size dependence during the development of the amphibian foot. Colchicine-induced digital loss and reduction. J Embryol Exp Morphol. 1983; 76:177–197. [PubMed: 6631320]

28. Thornton CS. The effect of colchicine on limb regeneration in larval amblystoma. Journal of Experimental Zoology. 1943; 92(3):281–295.

29. Whited JL, Lehoczky JA, Tabin CJ. Inducible genetic system for the axolotl. Proc Natl Acad Sci U S A. 2012; 109(34):13662–13667. [PubMed: 22869739]

30. Kragl M, et al. Cells keep a memory of their tissue origin during axolotl limb regeneration. Nature. 2009; 460(7251):60–65. [PubMed: 19571878]

Highlights

- Repeated blastema removal exhausts axolotl limb regeneration, leading to amelia.
- Axolotl limbs that form after prolonged bud removal are miniaturized.
- Miniaturized axolotl limbs are nerve-deficient.
- Miniaturized limbs can be used to study size determination during regeneration.

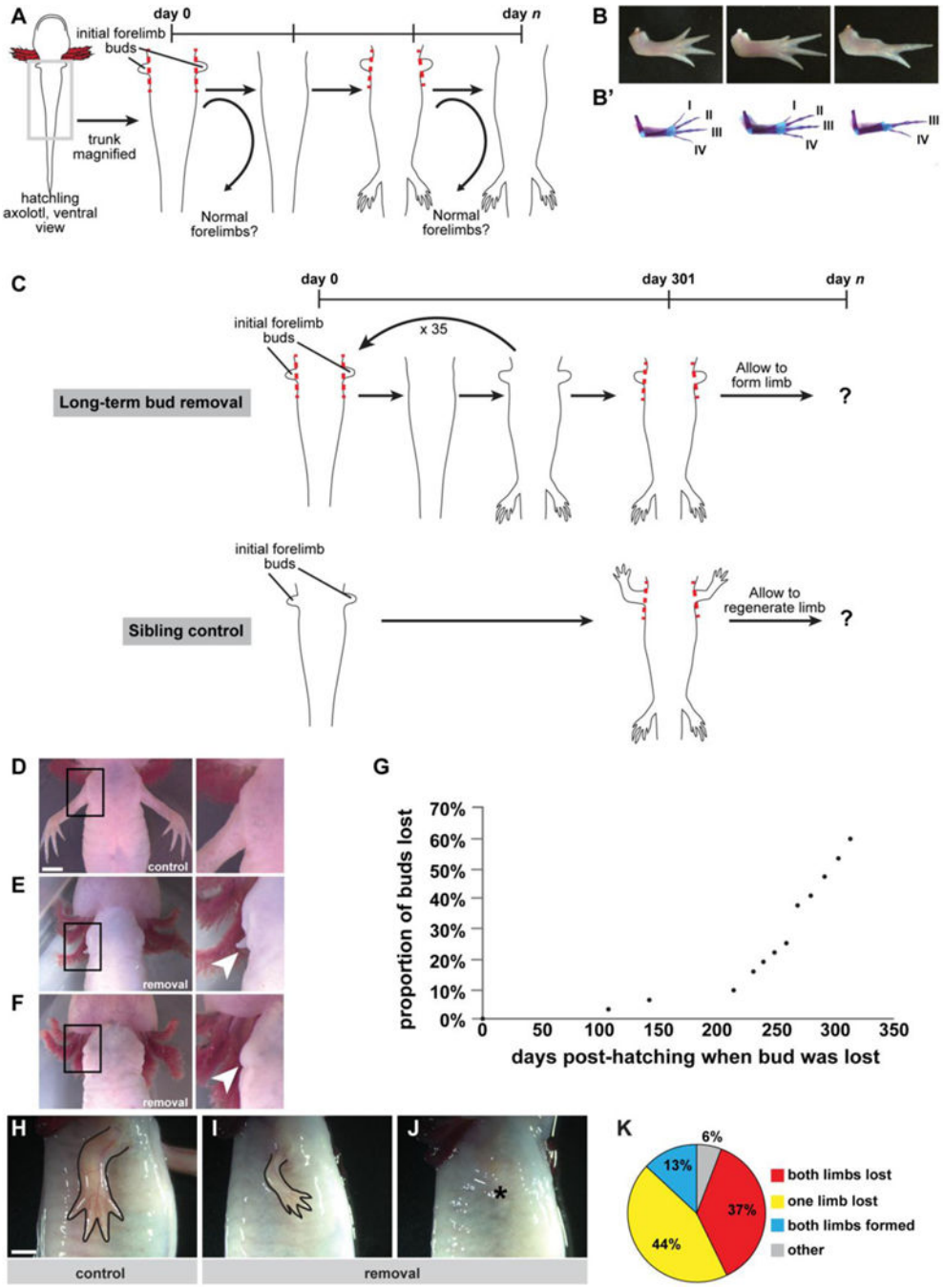

Figure 1. Experimental design and gross morphological outcomes after repeated bud removal

We performed two primary lines of experimentation: 1) short-term bud removal (i.e. up to 10 removals) with animal drop out and 2) long-term bud removal (i.e. 36 removals) without dropout. (A) Schematic of short-term bud removal experiments. Dashed red lines indicate cutting plane. Curved arrows indicate that animals are dropped out of the experimental protocol at select time points and then allowed to grow a limb. (B) Dorsal view of representative limb morphologies observed when limb formation is delayed. Anterior is at top and posterior is at bottom of the image. (B') Dorsal view of skeletal preparations of

limbs shown in (B). Digit identity is noted with Roman letters. (C) Schematic of long-term bud removal experiments. Dashed red lines indicate cutting plane. Control siblings were amputated proximally at the time of the last bud removal. Both control animals and animals that underwent repeated bud removal were allowed to fully form limbs after these final procedures. (D) Representative example of control limbs from a sibling of the exact same age as the experimental animals, ventral view, right forelimb/body junction (area inside black box) magnified at right. (E) Representative example of a reformed bud-like structure (arrowhead in magnified inset) on an experimental animal following 11 days of growth since last removal. (F) Representative example of loss of bud-like structure (arrowhead in magnified inset) following repeated removal, imaged 11 days after last removal. (G) Cumulative distribution plot of loss of bud-like structure as a function of time (n=32 buds/16 animals). (H–J) Representative examples of morphological outcomes when primary limbs are allowed to form at 313 days post-hatching, lateral view of right forelimb. (H) Sibling control amputated at the same time point, 313 days post-hatching, and allowed to regenerate for ~16 weeks (n= 26 forelimbs/13 animals). (I) Example outcome in an experimental animal allowed to form a fully patterned/differentiated limb, beginning at 313 days post-hatching (n=12/32 forelimbs). (J) Example outcome in an experimental animal which lost the ability to regrow a limb during the course of the study (n=19/32 forelimbs). Asterisk indicates shoulder joint. (K) Quantification of final outcomes in experimental animals (Both limbs lost: n=6/16 animals; one limb lost: n=7/16 animals; both limbs formed: n=2/16; other: n=1/16). Scale bars are 5 mm; bar in (D) applies to (D–F); bar in (H) applies to (H–J).

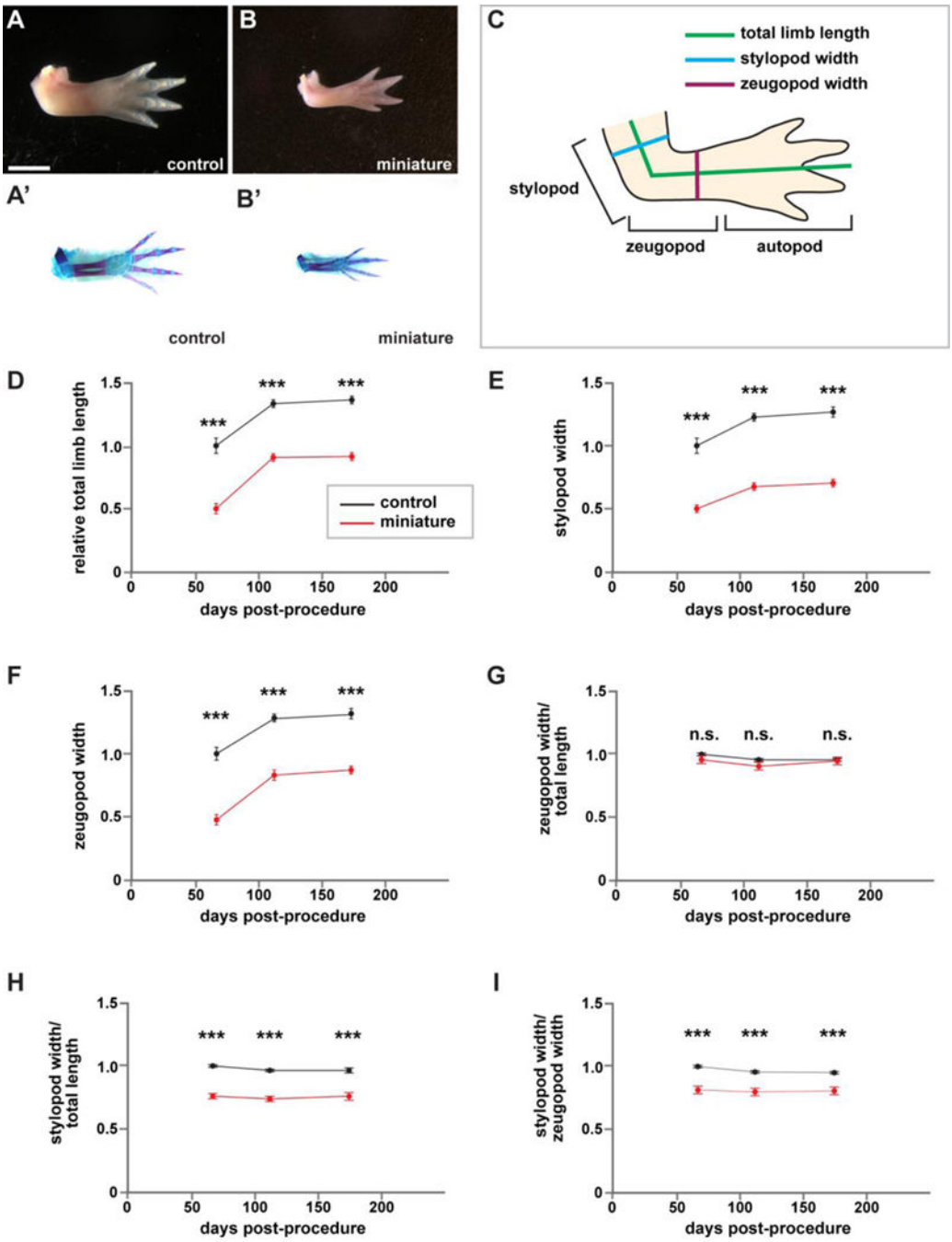

Figure 2. Miniaturized limbs are structurally normal

Structural and morphological analysis of miniaturized and control limbs. If an animal had two forelimbs, then the measurements of the two limbs were averaged to generate a single measurement for each animal. (A–B) Representative whole-mount images of control (A) and miniature limbs (B), dorsal view, anterior at top. (A'–B') Skeletal preparations of corresponding limbs in (A–B). (C) Schematic for quantifications. (D–I) Quantification of limb attributes over time, normalized to sibling controls at 66 days post-procedure (amputation for control siblings, last removal of bud-like structure for miniature limbs).

N=13 control animals; n=10 animals with miniaturized limbs. (D) Total limb length. (E) Stylopod width. (F) Zeugopod width. (G) Stylopod width/total length. (H) Zeugopod width/total length. (I) Stylopod width/zeugopod width. Measurements are mean +/− s.e.m., ***adjusted p-val<0.001, n.s. not significant. A two-way repeated measures ANOVA was used to test differences between groups and time. Post-hoc analyses using Bonferroni's Multiple Comparisons Test were performed to test differences between control and mini-limbs at each time point and to adjust for multiple comparisons. Scale bar refers to images (A–B') and is equal to 5 mm.

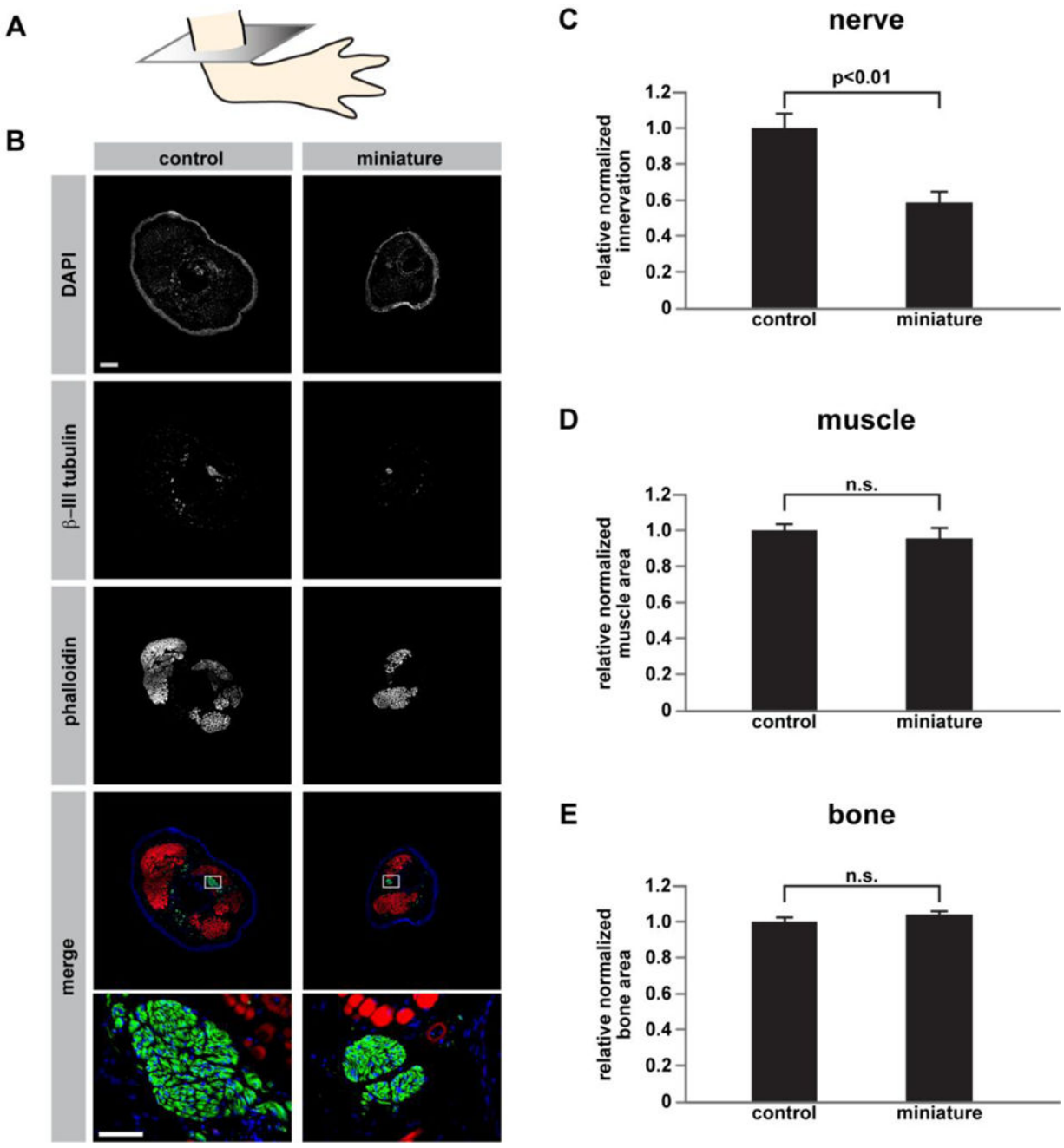

Figure 3. Miniaturized limbs are nerve deficient

(A) Schematic showing the plane through which limbs were sectioned, mid-stylopod, at 16 μm, for staining. (B) Representative immunofluorescent images from control limbs (left column) and miniature limbs (right column) stained with DAPI, βIII-tubulin, and phalloidin. Bottom-most panels are higher magnification views of areas enclosed in boxes outlined in the merged images. (C) Quantification of nerve area relative to total cross-sectional area (n=4 biological replicates for each group; $p<0.01$). (D) Quantification of muscle area relative to total cross-sectional area (n=4 biological replicates for each group). (E) Quantification of bone area relative to total cross-sectional area (n=4 biological replicates for each group). A

two-tailed t-test was used to determine significance for the comparisons in (C–E). Measurements are mean +/−s.e.m. Scale bar in (B) refers to all images except the bottom two images and is 500 μm. Scale bar in bottom image of (B) refers to high magnification images and is 100 μm.

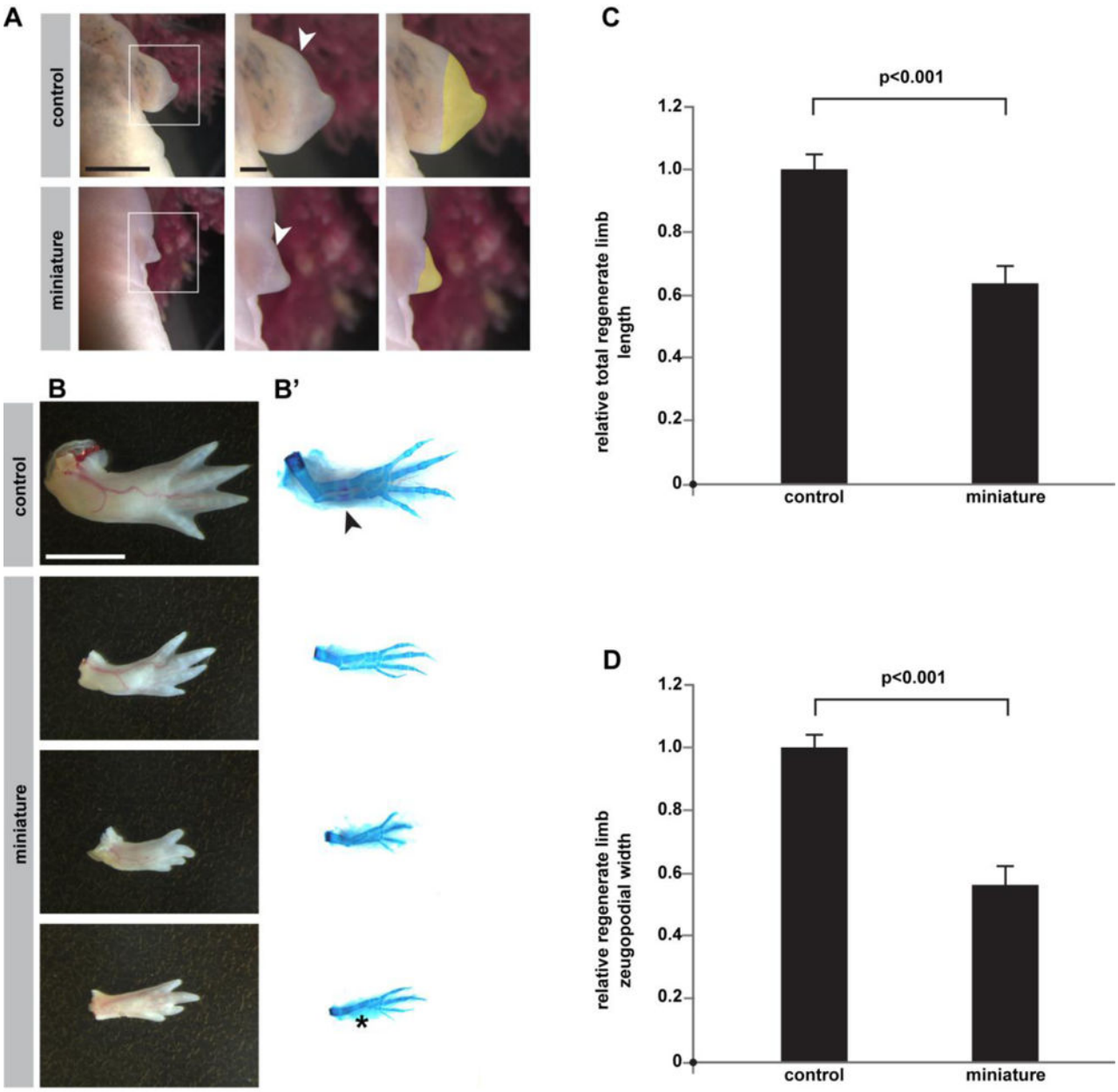

Figure 4. Miniaturized limbs regenerate small limbs following amputation

Morphological analysis of miniature and control limbs following amputation. (A) Representative images of blastemal formation at 23 days post-amputation. White arrowheads indicate the plane of amputation plane, and yellow highlights indicate each blastema's area. (B–B') Dorsal view of representative morphological outcomes at ~11 weeks post-amputation. Left column (B) is whole-mount, and right column (B') is skeletal preparation of same limbs. Arrow indicates ossification in control. Asterisk indicates loss of ulna. (C–D) Quantification of regenerated limb sizes (n=12 control animals/24 forelimbs; n=8 mini-limb animals/10 forelimbs). (C) Total relative regenerate limb length ($p<0.001$). (D) Relative zeugopodial width ($p<0.001$). Measurements are mean +/− s.e.m. A two-tailed t-test was used to assess significance. Scale bar in top-left image of (A) equals 5 mm and applies to

left-most images. Scale bar in top-middle image of (A) is 1 mm and applies to middle and right-most images. For (B), scale bar equals 5 mm. The miniature limbs challenged to regenerate in this figure were formed after 36 bud removals.